

EECS 442: Computer Vision

Digital Image Correlation

Final Report

Sravan Balaji
University of Michigan
balajsra@umich.edu

Kevin Monpara
University of Michigan
monpara@umich.edu

Abstract

Material properties for metal specimens are typically conducted using traditional strain gauges during tensile tests. However, using Digital Image Correlation (DIC), these properties can be calculated with the correct setup and a series of images as the metal is being pulled. The goal of this project was to be able to calculate material properties like Poisson's ratio, Young's modulus, ultimate tensile strength, and yield strength as well as plot a stress-strain curve using a images provided to us by John Laidlaw, Professional Engineer at the University of Michigan Mechanical Engineering department. We were mostly successful in reaching our goal. Furthermore, we were able to see strains at different points in the specimen and predict where it was going to break.

1. Introduction

Performing tensile tests on materials is necessary to be able to calculate important properties such as Poisson's ratio, Young's modulus, ultimate tensile strength, and yield strength. These properties are important because they are necessary considerations when building machinery or structures out of them. Typical tensile tests use physical strain gauges that have to be attached to the specimen with an adhesive. This device increases in resistance as the strain increases, so a voltage signal can be used to measure strain. There has been an increased interest in using non-contact methods to calculate strain in the field of mechanical and structural engineering. The main reason for this increased interest is that complex lab setups with physical gauges can't be used in the real world to monitor stress and strain of structures, especially when one is interested in very small or very large scale deformations.

Digital Image Correlation (DIC) has become more prominent as a non-contact method of measuring strain. DIC is a method where a material can be monitored as it de-

forms under stress. A grid of points are tracked via template matching as they are displaced and warped in the material. Using a series of images, these displacement distances can be used to calculate strain, Poisson's ratio, Young's modulus, ultimate tensile strength, and yield strength by creating a stress-strain curve.

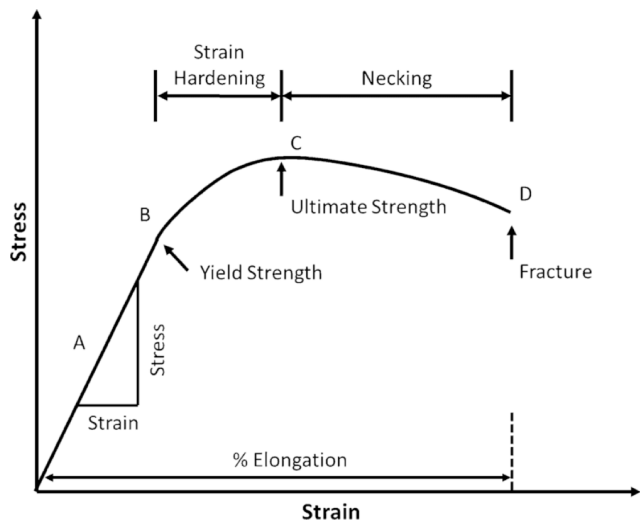


Figure 1. Reproduced from [4]. A stress-strain curve describes how a material behaves under increasing strain. This curve can be used to find Yield Strength (when necking occurs), Ultimate Tensile Strength (maximum sustainable tensile load), and Fracture Strength (when the material will fracture). Additionally, the slope of the initial elastic region is Young's modulus (ratio of stress required to achieve a certain strain in the specimen).

For our project, we wanted to implement DIC to generate a stress-strain curve and be able to visualize strain concentrations in the specimen as it was being pulled. We were able to get access to the data we needed from John Laidlaw, Professional Engineer at the University of Michigan Mechanical Engineering department. The data contains 702 images of a brass specimen (one shown below) undergoing

a tensile test. To determine the quality of our results, we can see if our calculated material properties match up with the accepted values and see if we are able to determine where a fracture point will be from the strain fields.

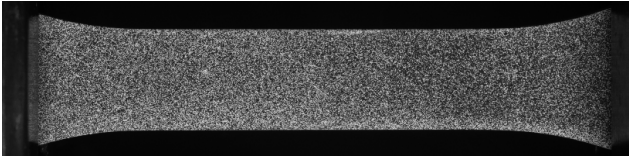


Figure 2. An image taken of a brass specimen undergoing a tensile test. Provided by John Laidlaw, Professional Engineer at the University of Michigan Mechanical Engineering.

2. Approach

2.1. General Steps

Digital Image Correlation works by tracking subsets of an image and calculating how much it moves from one image to the next. We had a series of 702 images taken of a brass specimen as it was being pulled, and the goal was to track small displacements of different points of the specimen as it was under going a tensile test. This was possible because the camera was fixed in place. The general steps are listed below:

1. Select image N and $N+1$
2. Split image N into subsets
3. Match subsets in image N to subsets in image $N+1$ with matchTemplate OpenCV function [5]
4. Find displacement between matching subsets in subsequent images
5. Create displacement field to visualize regions of high and low displacement
6. Create strain field from displacement field using a spatial derivative
7. Repeat steps 1-6 for all images
8. Plot stress and strain curve
9. Calculate material properties

Figure 4 shows how template matching works to find displacement.

2.2. Speckle Patterning

To track unique areas of the specimen, template matching needs a unique pattern to recognize [3]. In DIC, the specimen is patterned with random paint speckles. A zoomed in image of the pattern can be seen in Figure 3 on the right.

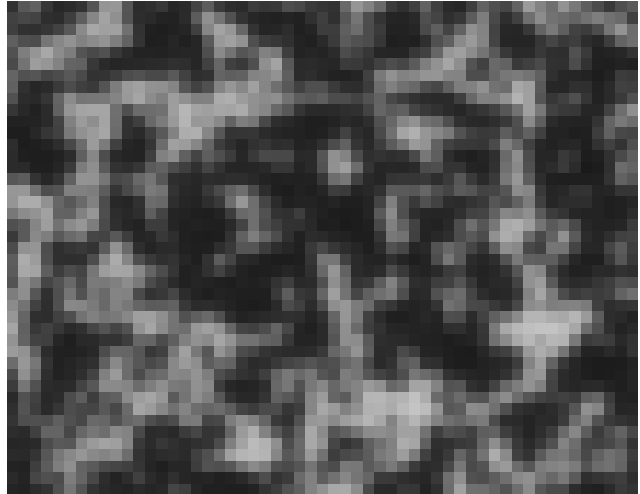


Figure 3. Zoomed in image showing the speckled pattern on the brass specimen. This can be used to find matching subsets in subsequent images to track displacement.

2.3. Template Matching

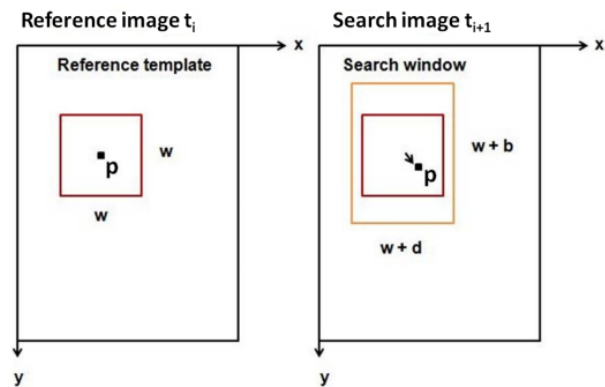


Figure 4. Reproduced from [6]. Displacements are found using template matching. We take a subset in the reference image and compare it to the subsets around the same position (search window) in the search image to find the best match.

Template matching looks for a reference subset inside of a search window in the search image. We use template matching to see how the specimen warps from one image to the next. To find the displacement (how much the material has been stretched), we take a reference template, create a surrounding search window in the search image, and look for the reference template in the window. Depending on where we find it, we can easily get its displacement in that area. There are a few different template matching methods available from OpenCV. In Section 4, Implementation Details, we will outline how we picked the best template matching method for our data.

2.4. Calculations

The math behind creating a stress-strain curve is fairly straightforward. We will be using the following equations:

$$\sigma = F/A \quad (1)$$

where σ is axial stress in MPa, F is axial force in N, and A is cross-sectional area in mm^2 .

$$\epsilon = (l - l_0)/l_0 \quad (2)$$

where ϵ is axial strain (unitless), l is the elongated length in mm, l_0 is the original length in mm.

$$E = \sigma/\epsilon \quad (3)$$

where E is Young's Modulus in GPa. We can then construct the curve and calculate ultimate tensile strength, and yield strength. From a plot of transverse vs. axial strain, we can estimate Poisson's ratio.

3. Results

3.1. Displacement and Strain Fields

We were able to generate a displacement field for every N and $N+1$ images. Early on, we can see that the displacement is quite small as we would expect. However, as the force increases in the tensile test, the displacement increases. Some areas experience a greater displacement than others, as shown in the following figures. From inspection, we found that this was consistent with how the material actually deforms as it undergoes the tensile test.

We can also see areas of high strain in certain images. For example, right before the specimen fractures, we see high strain along the line where the crack forms. This is extremely useful for real world applications where one might be concerned with identifying potential failure points.

The displacement and strain fields are shown in Figures 7, 8, 9, 10, 11, and 12 on the following pages.

3.2. Stress-Strain Curve

Using the numerical data provided, we plotted displacement, load, and stress over time. This is shown in Figure 5. Using the load, displacement, and cross-sectional area, we generated the stress-strain curve at the top of Figure 6. Using DIC, we tracked the displacement of two points on the brass specimen through subsequent images to determine axial and transverse strains. Stress determined from the numerical data and the axial strain from DIC are shown in the bottom plot of Figure 6. The top plot uses the displacement of the ends of the specimen while the bottom plot uses the displacement of points along the gauge length, thus producing more accurate strains in the region of interest (where the crack forms).

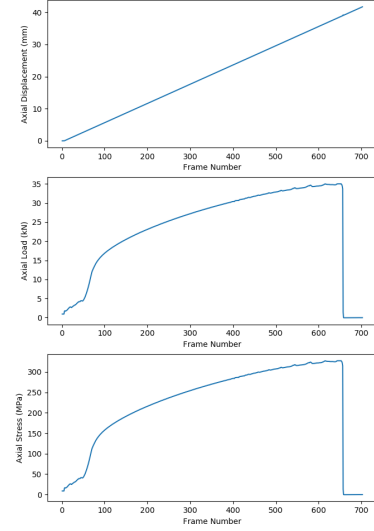


Figure 5. Plots of displacement, load, and stress from provided numerical data.

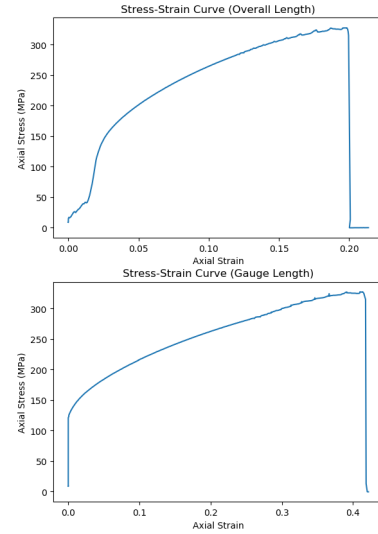


Figure 6. (Top) Stress-strain curve from provided numerical data using overall length displacement. (Bottom) Stress-strain curve from DIC on gauge length displacement.

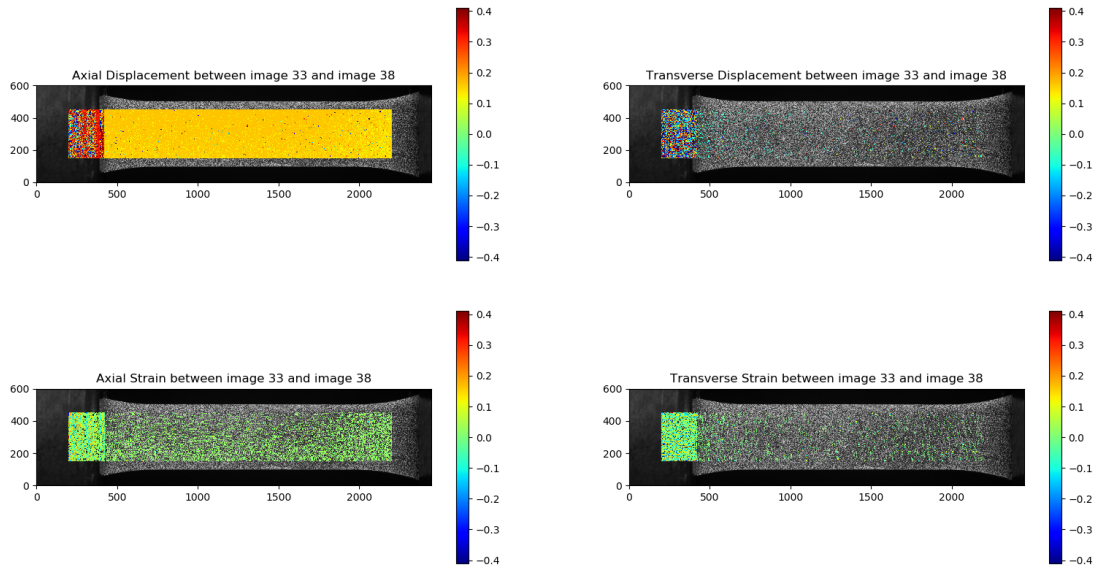


Figure 7. Displacement and Strain fields from Image 33 to 38 show what appears to be fairly constant displacement resulting in somewhat random strain measurements.

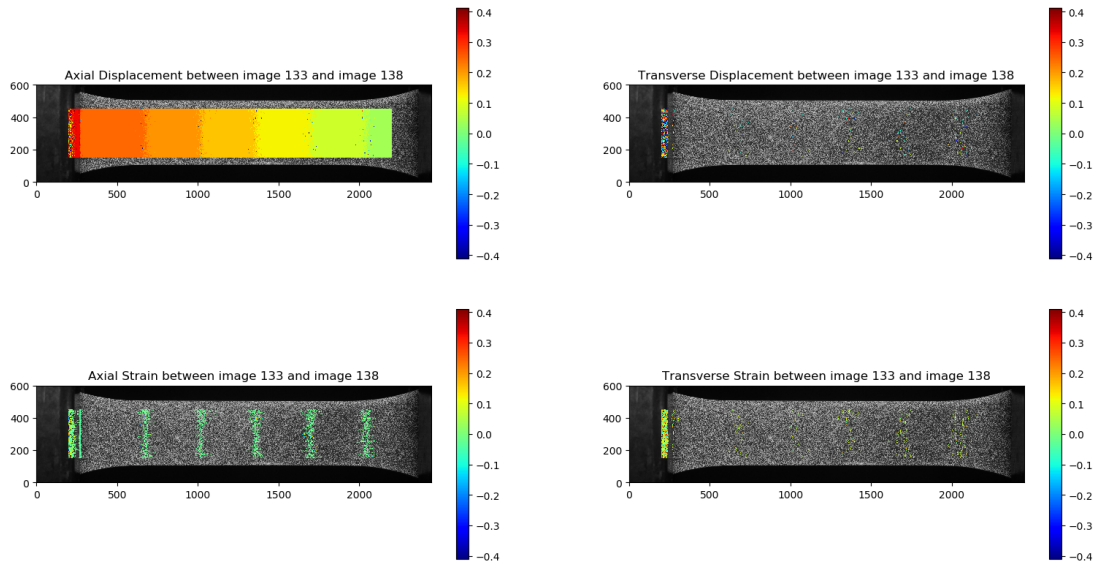


Figure 8. Displacement and Strain fields from Image 133 to 138 show some regions of displacement are larger than others, resulting in strain bands appearing in the axial strain plot.

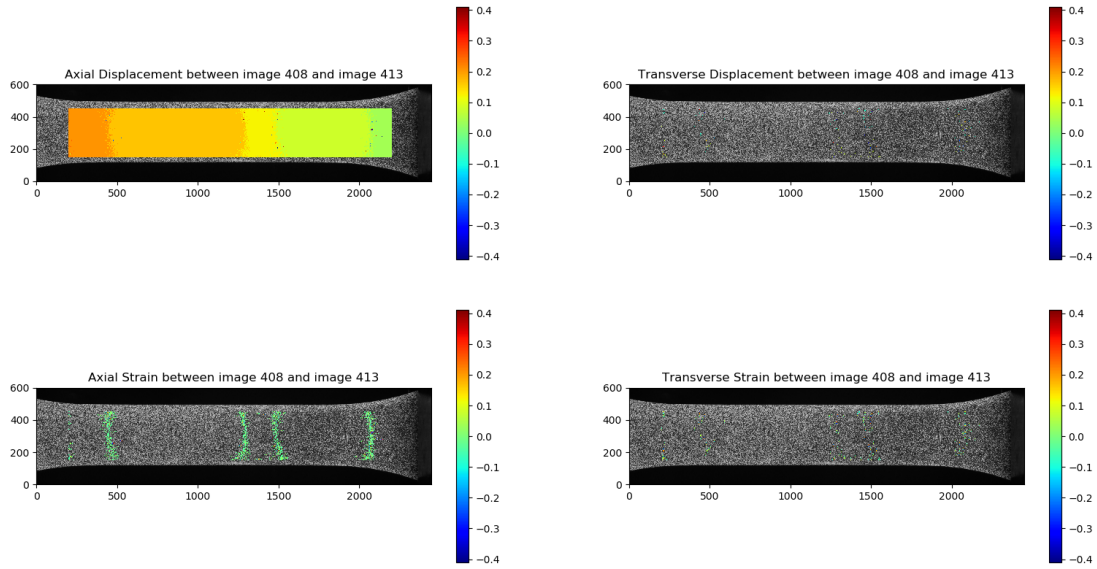


Figure 9. Displacement and Strain fields from Image 408 to 413 show that the strain bands appear curved, indicating that the axial strain changes along the transverse axis.

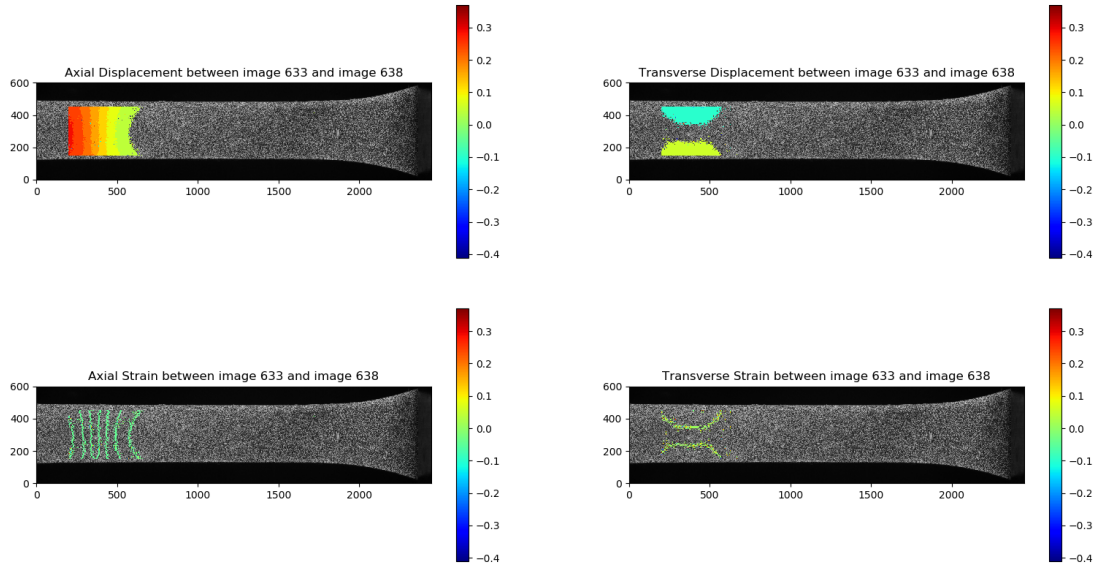


Figure 10. Displacement and Strain fields from Image 633 to 638 show that the horizontal strain bands have become much more compressed and we now see displacement and strain in the transverse direction, indicating that necking is occurring.

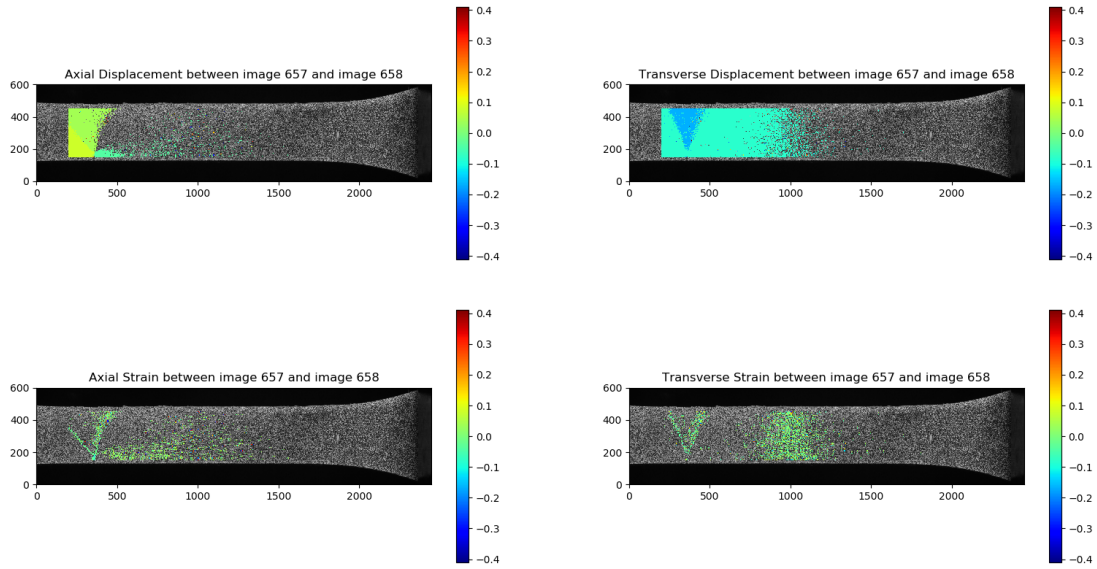


Figure 11. Displacement and Strain fields from Image 657 to 658 show a shearing effect in the displacement and strain fields indicating that fracture will occur along this line.

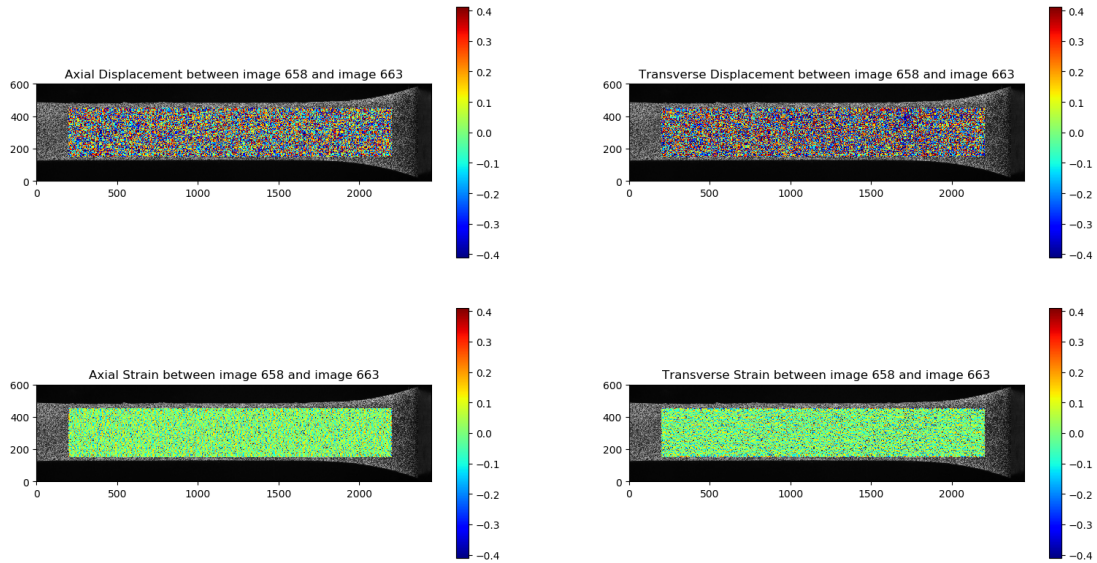


Figure 12. Displacement and Strain fields from Image 658 to 663 show that the template matching fails once the specimen fractures since the displacements are very fast and large.

3.3. Yield Strength

From the top plot on Figure 6 we see that the yield strength is approximately 150 MPa. From the bottom plot on Figure 6 we see that the yield strength is approximately 125 MPa. Accepted yield strength for brass ranges from 95 - 500 MPa, so this is reasonable.

3.4. Ultimate Tensile Strength

From both plots on Figure 6 we see that ultimate tensile strength is not readily apparent. It appears that the ultimate tensile strength and fracture strength are both around 325 MPa. Accepted values range from 310 - 550 MPa, so this is reasonable.

3.5. Young's Modulus

Young's modulus is very inaccurate on our plot due to the resolution limitations of our implementation of DIC. Many commercial methods use interpolation between pixels to achieve sub-pixel resolution, so they are able to produce more data points and get a clearer picture of the initial linear elastic region. We did not have enough points in the elastic region to get an accurate prediction of Young's modulus.

3.6. Poisson's Ratio

Poisson's ratio is also very inaccurate using our method. We expect the plot to have a negative slope, but due to our resolution limitations, our plot cannot really be used. The strain in the transverse direction is so small throughout the process that we could not accurately track it at the two points we selected to generate this plot.

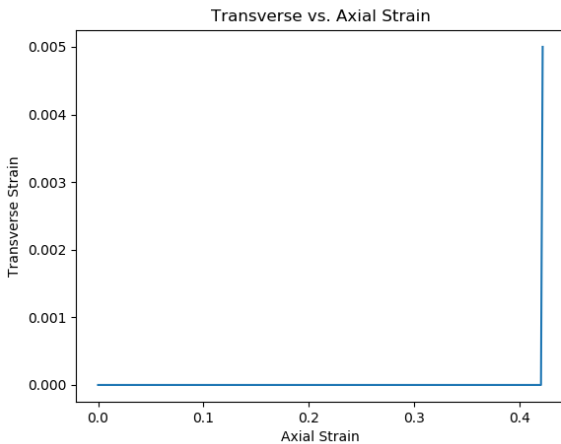


Figure 13. Poisson's ratio plot cannot be used because we expect a negative slope, but instead get nonsensical data due to the small transverse strains and resolution limitations.

4. Implementation Details

4.1. Template Matching Techniques

The main difficulty in DIC is template matching. OpenCV provides a `matchTemplate` [5] function that can find the best matching position of a template in an image using any of the methods shown in Figure 14.

1. `method=CV_TM_SQDIFF`

$$R(x, y) = \sum_{x', y'} (T(x', y') - I(x + x', y + y'))^2$$
2. `method=CV_TM_SQDIFF_NORMED`

$$R(x, y) = \frac{\sum_{x', y'} (T(x', y') - I(x + x', y + y'))^2}{\sqrt{\sum_{x', y'} T(x', y')^2 \cdot \sum_{x', y'} I(x + x', y + y')^2}}$$
3. `method=CV_TM_CCORR`

$$R(x, y) = \sum_{x', y'} (T(x', y') \cdot I(x + x', y + y'))$$
4. `method=CV_TM_CCORR_NORMED`

$$R(x, y) = \frac{\sum_{x', y'} (T(x', y') \cdot I(x + x', y + y'))}{\sqrt{\sum_{x', y'} T(x', y')^2 \cdot \sum_{x', y'} I(x + x', y + y')^2}}$$
5. `method=CV_TM_CCOEFF`

$$R(x, y) = \sum_{x', y'} (T'(x', y') \cdot I'(x + x', y + y'))$$

where

$$T'(x', y') = T(x', y') - 1/(w \cdot h) \cdot \sum_{x'', y''} T(x'', y'')$$

$$I'(x + x', y + y') = I(x + x', y + y') - 1/(w \cdot h) \cdot \sum_{x'', y''} I(x + x'', y + y'')$$
6. `method=CV_TM_CCOEFF_NORMED`

$$R(x, y) = \frac{\sum_{x', y'} (T'(x', y') \cdot I'(x + x', y + y'))}{\sqrt{\sum_{x', y'} T'(x', y')^2 \cdot \sum_{x', y'} I'(x + x', y + y')^2}}$$

Figure 14. Reproduced from [5]. The six matching methods available in the OpenCV function `matchTemplate`.

There are other methods that can be used, but they are not available in OpenCV. For the sake of time, we tested only the OpenCV methods on our data to see if points were being tracked accurately and reasonably well. Below in Figures 15 and 16 are results showing how well points were being tracked using each method.

We can see that Normalized Cross Correlation produces the most accurate tracking and least amount of outliers. To restrict the occurrence of outliers, we limited our search window size because we know that a point will not move more than a couple pixels per image.

Another consideration was runtime of the different methods. We found that most of the methods had around the same runtime, but Normalized Cross Correlation was slightly faster on average. More testing may produce different results.

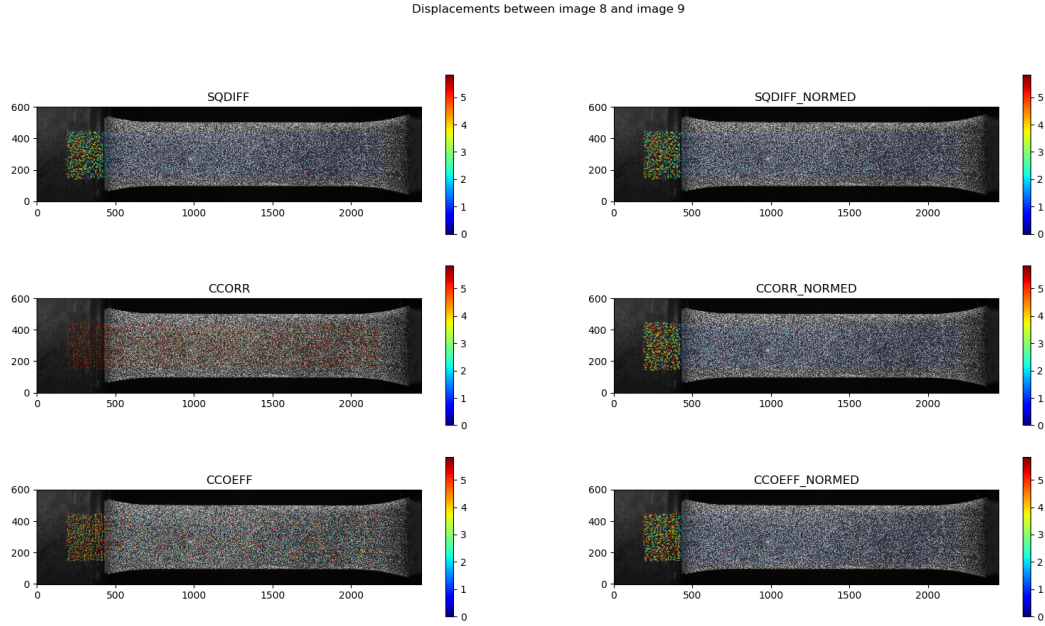


Figure 15. Comparison of OpenCV matching methods for displacement from image 8 to 9 shows that CCORR and CCOEFF result in very high, unreasonable displacements. The other four methods produce reasonable results with displacements close to 0 pixels.

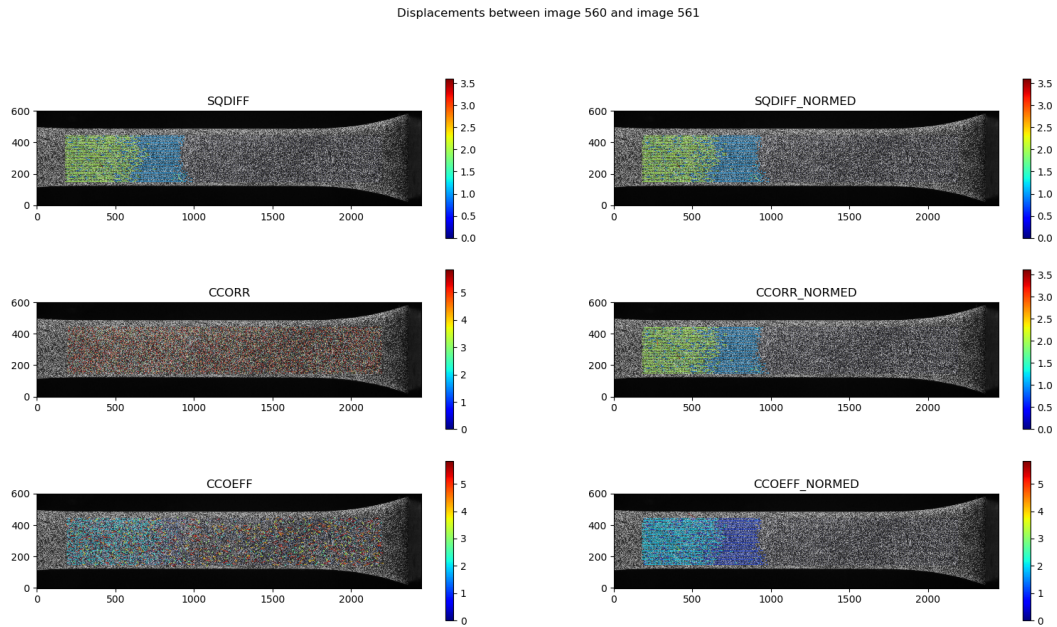


Figure 16. Comparison of OpenCV matching methods for displacement from image 560 to 561 shows that CCORR and CCOEFF still do not produce reasonable results. We now see that CCOEFF_NORMED differs from the remaining three methods. It has a higher range of displacements, up to 5 pixels in some places, which is unreasonable.

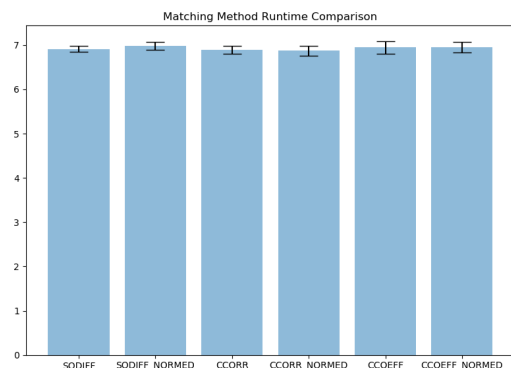


Figure 17. Comparison of OpenCV matching method runtimes shows that they all run in a similar amount of time, but Normalized Cross Correlation was slightly faster on average.

4.2. Choosing Parameters

Choosing subset size and search window sizes was difficult. As subset size decreases, the higher the resolution, but slower the processing time [2]. Window size depends on how much subsets move from one image to another. Choosing a proper subset size and search window size was mostly by trial and error until we found reasonable results. According to [1], “the fact that displacements in beam-like geometries tend to have linear gradients can be used to improve the accuracy of the measurements, because it minimizes the introduction of spurious noise arising from digital differentiation”. Similarly, we used the expectation that subsets would only displace a couple of pixels between subsequent images to limit the size of our search window. This improved runtime significantly and reduced noise.

Another parameter we had to adjust was the number of images ahead of the reference image that we should compare. In other words, should we compare the image N with image $N+1$ or should we compare image N with image $N+5$? Sometimes, choosing images too similar to each other resulted in movements less than a pixel. If we chose images too far apart, template matching was less accurate and prone to error. We compared N and $N+1$ for our calculations of stress and strain so that we have as many data points as possible and are accurate as possible. For our visualizations where qualitative results are needed, we compared N and $N+5$ images so that displacements and strains are larger and the difference in displacement magnitude is more pronounced.

5. Conclusion

Digital Image Correlation can be used to determine the strain on different materials in a non-contact way. Although sometimes limiting, we learned that DIC is a powerful way

to get qualitative images of high strain regions in a structure. These visualizations can be used in a variety of applications, both in the real world and in the confines of a lab or classroom.

References

- [1] J. M. Gorman and M. D. Thouless. The use of digital-image correlation to investigate the cohesive zone in a double-cantilever beam, with comparisons to numerical and analytical models. *Journal of the Mechanics and Physics of Solids*, 123:315–331, feb 2019.
- [2] J. Laidlaw. *Digital Image Correlation: An Overview*.
- [3] W. LePage. A practical guide to dic, apr 2019.
- [4] H. Lim and S. Hoag. Plasticizer effects on physical-mechanical properties of solvent cast soluplus films. *AAPS PharmSciTech*, 14, may 2013.
- [5] opencv dev team. Template matching, apr 2019.
- [6] R. Ravanelli, A. Nascetti, M. Di Rita, V. Belloni, D. Mattei, N. Nistico, and M. Crespi. A new digital image correlation software for displacements field measurement in structural applications. *The International Archives of the Photogrammetry, Remote Sensing and Spatial Information Sciences*, XLII-4/W2:140, jul 2017.